Inorganic Chemistry
Article

Syntheses and Structural, Physical, and Theoretical Studies of the Novel Isostructural Mo$_9$ Cluster Compounds Ag$_{2.6}$CsMo$_9$Se$_{11}$, Ag$_{4.1}$ClMo$_9$Se$_{11}$, and h-Mo$_9$Se$_{11}$ with Tunnel Structures

Patrick Gougeon* and Michel Potel

Laboratoire de Chimie du Solide et Inorganique Moléculaire, UMR CNRS 6511, Université de Rennes 1, Institut de Chimie de Rennes, Avenue du Général Leclerc, 35042 Rennes Cedex, France

Régis Gautier

Laboratoire de Physicochimie, UPRES 1795, Ecole Nationale Supérieure de Chimie de Rennes, Institut de Chimie de Rennes, Campus de Beaulieu, 35700 Rennes, France

The new isostructural compounds Ag$_{2.6}$CsMo$_9$Se$_{11}$ (**1**) and Ag$_{4.1}$ClMo$_9$Se$_{11}$ (**2**) were prepared by solid-state reaction in evacuated sealed silica tubes at 1200 °C and 860 °C, respectively. By topotactic reduction−oxidation reaction of Ag$_{4.1}$ClMo$_9$Se$_{11}$ with I$_2$, we also obtained the metastable compound h-Mo$_9$Se$_{11}$ (**3**). The three compounds crystallize in the hexagonal space group $P6_3/m$, $Z = 2$, (**1**) $a = 10.0472(2)$ Å, $c = 11.9548(2)$, (**2**) $a = 10.0321(2)$ Å, $c = 11.8734(2)$ Å, and (**3**) $a = 9.4204(2)$ Å, $c = 12.1226(2)$ Å. Their crystal structures were determined from single-crystal X-ray diffraction data and consist of interconnected Mo$_9$Se$_{11}$ units forming an original and unprecedented three-dimensional framework in which large tunnels are occupied randomly by a part of the Ag$^+$ and the Cl$^-$ ions in **2** and the Cs$^+$ ions in **1**, the remaining Ag$^+$ in **1** being localized in mirror planes around the 3-fold axis. First-principle calculations allow the understanding of the variation of the atomic distances. Electrical resistivity measurements carried out on single crystals of Ag$_{2.6}$CsMo$_9$Se$_{11}$ and Ag$_{4.1}$ClMo$_9$Se$_{11}$ in which the number of electrons per Mo$_9$ cluster is different indicate that the former is semiconducting whereas the latter is semimetallic.

Introduction

Inorganic compounds containing low-valent molybdenum are generally characterized by metal clusters of diverse sizes and geometries. Chalcogenide compounds containing octahedral Mo$_6$ clusters[1] are the most abundant and present interesting physical properties.[2,3] Molybdenum clusters with nuclearity higher than six such as Mo$_9$,[4] Mo$_{12}$,[5] Mo$_{15}$,[6] Mo$_{18}$,[7] Mo$_{21}$,[8] Mo$_{24}$,[9] Mo$_{30}$,[9] and Mo$_{36}$[10] can also be obtained and result from the one-dimensional trans-face sharing of Mo$_6$ octahedra. Among the latter clusters, the bioctahedral Mo$_9$ cluster is present alone or with other clusters of different nuclearity in a large number of compounds. For example, in the series Rb$_{2n}$(Mo$_9$S$_{11}$)(Mo$_{6n}$S$_{6n+2}$) ($n = 1$ to 5),[11] the Mo$_9$ cluster cocrystallizes with Mo$_6$, Mo$_{12}$, Mo$_{18}$, Mo$_{24}$, or Mo$_{30}$ clusters. The Mo$_9$ cluster was first observed alone in Ag$_{3.6}$Mo$_9$Se$_{11}$[4] and more recently in K$_2$Mo$_9$S$_{11}$.[12] From the latter two compounds, it was possible to synthesize by topotactic reduction−oxidation reaction at low-temperature

---

* Author to whom correspondence should be addressed. E-mail: Patrick. Gougeon@univ-rennes1.fr.

(1) Chevrel, R.; Sergent, M. In *Superconducting in Ternary Compounds*; Fischer, Ø., Maple, M. B., Eds.; Springer-Verlag: Berlin, Heidelberg, New York, 1982; Part I.

(2) Fischer, Ø. *Appl. Phys.* **1978**, *16*, 1.

(3) Maple, M. B.; Fischer, Ø. In *Superconducting in Ternary Compounds*; Fischer, Ø., Maple, M. B., Eds.; Springer-Verlag: Berlin, 1982; Parts I and II.

(4) Gougeon, P.; Padiou, J.; Le Marouille, J.-Y.; Potel, M.; Sergent, M. *J. Solid State Chem.* **1984**, *51*, 218.

(5) (a) Gougeon, P.; Potel, M.; Padiou, J.; Sergent, M. *Mater. Res Bull.* **1987**, *22*, 1087. (b) Gautier, R.; Picard, S.; Gougeon, P.; Potel, M. *Mater. Res. Bull.* **1999**, *34*, 93.

(6) (a) Gougeon, P.; Potel, M.; Sergent, M. *Acta Crystallogr.* **1989**, *C45*, 182. (b) Gougeon, P.; Potel, M.; Sergent, M. *Acta Crystallogr.* **1989**, *C45*, 1413.

(7) Gougeon, P.; Potel, M.; Padiou, J.; Sergent, M. *Mater. Res. Bull.* **1988**, *23*, 453.

(8) Picard, S.; Gougeon, P.; Potel, M. *Acta Crystallogr.* **1997**, *C53*, 1519.

(9) Gougeon, P. Thesis, Rennes, 1984.

(10) Picard, S.; Gougeon, P.; Potel, M. *Angew. Chem.* **1999**, *38*, 2034.

(11) Picard, S.; Saillard, J.-Y.; Gougeon, Noël, H. P.; Potel, M. *J. Solid State Chem.* **2000**, *155*, 417.

(12) Picard, S.; Halet, J.-F.; Gougeon, P.; Potel, M. *Inorg. Chem.* **1999**, *38*, 4422.

---

isostructural compounds in which the number of electrons available for Mo−Mo bonding per Mo_9 cluster, often called metallic electrons (ME), was different and thus presented different electrical behaviors.[12,13] We describe here the synthesis and crystal structures of three isostructural compounds $Ag_{2.6}CsMo_9Se_{11}$, $Ag_{4.1}ClMo_9Se_{11}$, and $h\text{-}Mo_9Se_{11}$, which crystallize in a new structural type only based on the Mo_9 cluster and have different ME counts. The binary compound constitutes thus the archetype, and the quaternary compounds can be seen as filled $h\text{-}Mo_9Se_{11}$ variants. Electronic structures of these compounds have been investigated using density functional theory (DFT) calculations. The results are also presented as well as resistivity measurements performed on single crystals.

Experimental Section

Syntheses. Starting materials used for the solid-state syntheses were $MoSe_2$, $Cs_2Mo_6Se_6$, Ag, and Mo, all in powder form. Before use, Mo powder was reduced under H_2 flowing gas at 1000 °C during 10 h in order to eliminate any trace of oxygen. The molybdenum diselenide was prepared by the reaction of selenium with H_2 reduced Mo in a 2:1 ratio in an evacuated (ca. 10^{-2} Pa of Ar residual pressure) and flame-baked silica tube, heated at about 700 °C during 2 days. $Cs_2Mo_6Se_6$ was synthesized from an ion-exchange reaction of $In_2Mo_6Se_6$ with CsCl at 800 °C, as previously described.[14] All starting reagents were found monophasic on the basis of their powder X-ray diffraction diagram made on an Inel curve sensitive position detector CPS 120. Furthermore, in order to avoid any contamination by oxygen and moisture, the starting reagents were kept and handled in a purified argon-filled glovebox.

$Ag_{4.1}ClMo_9Se_{11}$. Single crystals of $Ag_{4.1}ClMo_9Se_{11}$ were initially synthesized in a reaction to grow single crystals of $Ag_{3.6}Mo_9Se_{11}$[4] by a chemical transport reaction in a silica tube fused under vacuum. The transporting agent was AgCl (ca. 150 mg for 1 g of $Ag_{3.6}Mo_9$-Se_{11}), and the temperatures at both ends of the tube were 860 and 960 °C. Quantitative microanalyses of the crystals thus obtained revealed the presence of chlorine and a composition corresponding to the formula $Ag_{4.11}Cl_{1.07}Mo_9Se_{10.95}$. The stoichiometry was confirmed by the structural study made by X-ray diffraction on one of the crystals as well as by the synthesis of a monophasic powder sample. The latter was obtained by heating the required stoichiometric mixture of AgCl, Ag, Mo, and $MoSe_2$ in an evacuated silica tube at 850 °C for 24 h. Reactions made with different stoichiometry in silver were also tested and did not lead to single-phase products. The isostructural $Ag_{4.1}BrMo_9Se_{11}$ compound was also synthesized. However, no single crystals could be obtained.

$Ag_{2.6}CsMo_9Se_{11}$. $Ag_{2.6}CsMo_9Se_{11}$ was first obtained as single crystals in an attempt to insert Ag in $Cs_2Mo_{12}Se_{14}$ at high temperature. As for $Ag_{4.1}ClMo_9Se_{11}$, the stoichiometry was only known after a complete structural study on a single crystal by X-ray diffraction. Subsequently, we could get a single-phase powder sample by heating the required stoichiometric mixture of Ag, Mo, $Cs_2Mo_6Se_6$, and $MoSe_2$ in an evacuated silica tube at 1200 °C during 12 h.

$h\text{-}Mo_9Se_{11}$. The binary compound was obtained by reaction of iodine on single crystals of $Ag_{4.1}ClMo_9Se_{11}$ in ethanol at 150 °C

for 48 h. The absence of silver and chlorine in the crystals thus synthesized was checked by qualitative microanalyses using a JEOL JSM-6400 scanning electron microscope equipped with an OXFORD energy-dispersive-type X-ray spectrometer and confirmed by the single-crystal structure determination.

Single-Crystal X-ray Studies. Black single crystals of $Ag_{2.6}$-$CsMo_9Se_{11}$ (**1**), $Ag_{4.1}ClMo_9Se_{11}$ (**2**), and $h\text{-}Mo_9Se_{11}$ (**3**) were selected for data collection. Intensity data were collected on a Nonius Kappa CCD diffractometer using graphite-monochromatized Mo Kα radiation ($\lambda = 0.71073$Å) at room temperature. The frames were recorded using $\Delta\omega = 1.7°$, 1.5°, and 1.2°, rotation scans with X-ray exposure times of 93s, 60s and 36s for **1**, **2**, and **3**, respectively. Reflection indexing, Lorentz−polarization correction, peak integration, and background determination were performed using the program DENZO[15] of the Kappa CCD software package.[16] Absorption corrections were applied either with the SORTAV program[17] or the Gaussian method.[18] All structure refinements and Fourier syntheses were carried out using SHELXL-97[19] or JANA2000.[20]

$Ag_{2.6}CsMo_9Se_{11}$. The crystal structure of $Ag_{2.6}CsMo_9Se_{11}$ was solved with the direct methods program SHELXS[19] in the $P6_3/m$ space group. A subsequent Fourier synthesis reveals the silver atoms and a quasi-continuous electron density along the c axis due to the caesium atoms. At this stage of the refinement, two different procedures were possible to describe the caesium distribution: a model with four caesium atom sites using second-order tensors for the anisotropic displacement parameters or a model with one caesium atom in (0, 0, 0.25) and use of anharmonic tensors up to the fourth order.[21] The latter model gave better results with no residual peak higher than 1.64 e/Å^3 in the channel instead of 3.494 e/Å^3 for the first model. The final refinement cycle of the anharmonic model converged to the values of $R = 0.0446$ and $R_w = 0.0446$. The final electron density difference map was flat with a maximum of 2.21 e/Å^3 and a minimum of -2.36 e/Å^3.

$Ag_{4.1}ClMo_9Se_{11}$. The initial positions for all the molybdenum and selenium atoms were determined with the direct methods program SHELXS[19] in the $P6_3/m$ space group. At this stage, an electron density difference map revealed the remaining atoms. The refinement of the positional and anisotropic displacement parameters for all atoms and occupancy factor parameters for the Ag and Cl sites led to the values of $R = 0.133$. Further inspection of the data reveals a twinning with the twin law 0 1 0, 1 0 0, 0 0 −1. Introduction of the twinning led to the final values R1 = 0.0352 and wR2 = 0.0731 and to the stoichiometry $Ag_{4.13(1)}ClMo_9Se_{11}$. The site occupancy factors for Ag4 and Cl located in the tunnels were 0.505(9) and 0.509(9) and thus were fixed to 0.5. The final electron density difference map was flat with a maximum of 2.309 e/Å^3 and a minimum of -2.827 e/Å^3. Attempts to refine the silver atoms using anharmonic atomic displacement parameters were unsuccessful.

(13) Gougeon, P.; Potel, M.; Padiou, J.; Sergent, M.; Boulanger, C.; Lecuire, J.-M. *J. Solid State Chem.* **1987**, *71*, 543.

(14) Potel, M.; Gougeon, P.; Chevrel, R.; Sergent, M. *Rev. Chim. Miner.* **1984**, *21*, 509.

(15) Otwinowski, Z.; Minor, W. In *Methods in Enzymology*; Carter, C. W., Jr., Sweet, R. M., Eds.; Academic Press: New York, 1997; Vol. 276, pp 307−326.

(16) Nonius (1998), COLLECT: KappaCCD software. Nonius BV: Delft, The Netherlands.

(17) Blessing, R. H. *Acta Crystallogr., Sect. A* **1995**, *51*, 33−38.

(18) Busing, W. R.; Levy, H. A. *Acta Crystallogr.* **1957**, *10*, 180−182.

(19) Programs for Crystal Structure Analysis (Release 97-2). Sheldrick, G. M., Institut für Anorganische Chemie der Universität, Tammanstrasse 4, D-3400 Göttingen, Germany, 1998.

(20) Petricek, V.; Dusek, M. *Jana2000*; Institute of Physics, Academy of Sciences of the Czech Republic: Prague, Czech Republic, 2000.

(21) (a) Bachman, R.; Schulz, H. *Acta Crystallogr.* **1984**, *40*, 668. (b) Zucker, U. H.; Schulz, H. *Acta Crystallogr.* **1982**, *38*, 563. (c) Kuhs, W. F. *Acta Crystallogr.* **1983**, *40*, 133.

Table 1. X-ray Crystallographic and Experimental Data for Ag$_{2.6}$CsMo$_9$Se$_{11}$, Ag$_{4.1}$ClMo$_9$Se$_{11}$, and h-Mo$_9$Se$_{11}$

	Ag$_{2.6}$CsMo$_9$Se$_{11}$	Ag$_{4.1}$ClMo$_9$Se$_{11}$	h-Mo$_9$Se$_{11}$
formula	Ag$_{2.6}$CsMo$_9$Se$_{11}$	Ag$_{4.1}$ClMo$_9$Se$_{11}$	h-Mo$_9$Se$_{11}$
fw, g mol^{-1}	2141.83	2212.97	1732.02
space group	$P6_3/m$	$P6_3/m$	$P6_3/m$
a, Å	10.0472(2)	10.0321(2)	9.4204(2)
c, Å	11.9548(2)	11.8734(2)	12.1226(2)
Z	2	2	2
V, Å^3	1045.11(3)	1034.88(3)	931.68(3)
ρ_{calcd}, g cm^{-3}	6.806	7.102	6.174
T, °C	20	20	20
λ, Å	0.71073	0.71073	0.71073
μ, mm^{-1}	28.401	28.515	27.308
R1[a]	0.0446	0.0352	0.0480
R_w[b] or wR2[c]	0.0446[b]	0.0731[c]	0.1041[c]

[a] R1 = $\sum||F_o| - |F_c||/\sum|F_o|$. [b] $R_w = \{\sum[w(|F_o| - |F_c|)^2]/\sum[wF_o^2]\}^{1/2}$. [c] wR2 = $\{\sum[w(F_o^2 - F_c^2)^2]/\sum[w(F_o^2)^2]\}^{1/2}$.

Table 2. Selected Interatomic Distances for Ag$_{2.6}$CsMo$_9$Se$_{11}$, Ag$_{4.1}$ClMo$_9$Se$_{11}$, and h-Mo$_9$Se$_{11}$

	Ag$_{2.6}$CsMo$_9$Se$_{11}$	Ag$_{4.1}$ClMo$_9$Se$_{11}$	h-Mo$_9$Se$_{11}$
intratriangle			
Mo1−Mo1 (×2)	2.6270(4)	2.6281(4)	2.6820(6)
Mo2−Mo2 (×2)	2.7423(6)	2.7362(5)	2.6838(9)
intertriangle			
Mo1−Mo2	2.6937(4)	2.7038(3)	2.7370(4)
Mo1−Mo2	2.7365(4)	2.7277(3)	2.7985(5)
intercluster			
Mo1−Mo1	3.6614(4)	3.6142(4)	3.2240(7)
Mo−Se			
Mo1−Se1	2.6035(7)	2.5984(4)	2.5909(6)
Mo1−Se1	2.6328(6)	2.6292(4)	2.6000(6)
Mo1−Se1$_{interunit}$	2.7130(4)	2.7011(3)	2.6090(6)
Mo1−Se2	2.6683(5)	2.6576(5)	2.7026(5)
Mo1−Se3	2.5439(5)	2.5389(5)	2.5234(7)
Mo2−Se1 (×2)	2.6408(5)	2.6510(3)	2.5357(5)
Mo2−Se2	2.5808(6)	2.5609(5)	2.5672(8)
Mo2−Se2	2.5902(5)	2.5737(5)	2.5893(8)
Ag1−Se1 (×2)	2.7935(5)	2.769(1)	
Ag1−Se2	2.6749(6)	2.623(1)	
Ag1−Se3 (×2)	2.8719(7)	3.005(3)	
Ag2−Se1 (×2)		2.6864(6)	
Ag2−Se2		2.615(1)	
Ag2−Cl		2.734(3)	
Ag3−Se1		2.761(5)	
Ag3−Se1		2.886(5)	
Ag3−Se1		2.912(5)	
Ag3−Cl		2.623(7)	
Ag4−Cl (×2)		2.516(7)	
Cs−Se1 (×6)	3.9859(4)		
Cs−Se2 (×3)	3.6790(6)		

h-Mo$_9$Se$_{11}$. Molybdenum and selenium atomic positions of Ag$_{4.1}$ClMo$_9$Se$_{11}$ were used in the first stage of the refinement. The final full-matrix least-squares refinement on F^2 which was based on a model including the positional and anisotropic displacement parameters for all atoms led to the values of R1 = 0.0480 and wR2 = 0.1041 for 1852 reflections with $I > 2\sigma(I)$. The final electron density difference map was flat with a maximum of 3.112 e/Å^3 and a minimum of −2.654 e/Å^3. In the tunnel, no peak higher than 1.63 e/Å^3 was observed, which rules out the presence of solvent or water molecules. This is also confirmed by the qualitative microanalyses.

The crystallographic and experimental data of the three compounds investigated are listed in Table 1, and selected interatomic distances in Table 2.

Electrical Resistivity Measurements. The studies of the temperature dependences of the electrical resistivity were carried out on single crystals of Ag$_{2.6}$CsMo$_9$Se$_{11}$ and Ag$_{4.1}$ClMo$_9$Se$_{11}$ using a conventional ac four-probe method with a current amplitude of 0.1 mA. Contacts were ultrasonically made with molten indium on single crystals previously characterized on a CAD-4 diffractometer. The ohmic behavior and the invariance of the phase were checked during the different measurements at low and room temperature.

Computational Procedure. Self-consistent ab initio band structure calculations were performed on the model compound Ag$_3$CsMo$_9$Se$_{11}$ and h-Mo$_9$Se$_{11}$ with the scalar relativistic tight-binding linear muffin-tin orbital (LMTO) method in the atomic spheres approximation including the combined correction.[22] Exchange and correlation were treated in the local density approximation using the von Barth−Hedin local exchange correlation potential.[23] Within the LMTO formalism interatomic spaces are filled with interstitial spheres. The optimal positions and radii of these additional "empty spheres" (ES) were determined by the procedure described in ref 24. Four and six non-symmetry-related ES with 0.79 Å ≤ r_{ES} ≤ 1.49 Å and 0.89 Å ≤ r_{ES} ≤ 2.46 Å were introduced for the calculations on Ag$_3$CsMo$_9$Se$_{11}$ and h-Mo$_9$Se$_{11}$, respectively. The full LMTO basis set consisted of 5s, 5p, 4d, and 4f functions for Mo and Ag spheres, 4s, 4p, and 4d for Se spheres, and s, p, d, and f functions for ES. The eigenvalue problem was solved using the following minimal basis set obtained from the Löwdin downfolding technique: Mo 5s, 5p, 4d; Ag 5s, 5p, 4d; Se 4s, 4p; and interstitial 1s LMTOs. The k space integration was performed using the tetrahedron method.[25] Charge self-consistency and the average properties were obtained from 224 irreducible k points for Ag$_3$CsMo$_9$Se$_{11}$ and h-Mo$_9$Se$_{11}$. A measure of the magnitude of the bonding was obtained by computing the crystal orbital Hamiltonian populations (COHP) which are the Hamiltonian population weighted density of states (DOS).[26] As recommended,[27] a reduced basis set (in which all ES LMTO's have been downfolded) was used for the COHP calculations. Bands, DOS, and COHP curves are shifted so that ϵ_F lies at 0 eV.
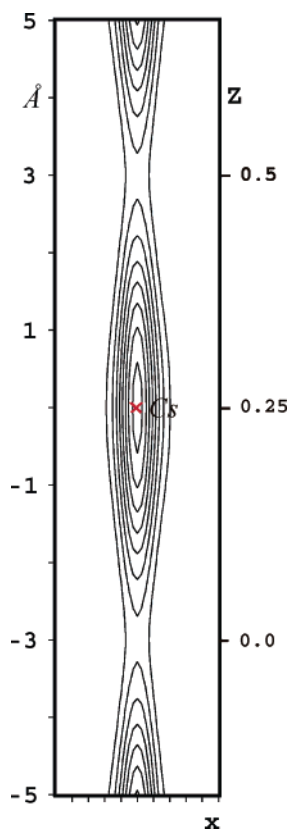
Results and Discussion

Crystal Structures. The h-Mo$_9$Se$_{11}$ archetype and the two filled variants Ag$_{2.6}$CsMo$_9$Se$_{11}$ and Ag$_{4.1}$ClMo$_9$Se$_{11}$ crystallize in a new structural type, the Mo−Se three-dimensional framework of which is based on interconnected Mo$_9$Se$_{11}$ clusters as illustrated in Figure 1 by the crystal structure of Ag$_{4.1}$ClMo$_9$Se$_{11}$. In Ag$_{2.6}$CsMo$_9$Se$_{11}$, only the Ag1 atoms are present, and the Cs atoms are delocalized along the c axis as shown by the probability density function map (Figure 2). The Mo$_9$Se$_{11}$ unit (Figure 3), which is centered on a 2d position ($^1/_3$, $^2/_3$, $^1/_4$) and thus has here the point symmetry C_{3h}, can be classically described as the result of the monoaxial face-sharing condensation of two Mo$_6$Se$_8$ units with loss of the Se atoms belonging to the shared faces. Such a unit can be also seen as the stacking of three planar Mo$_3$Se$_3$, instead of two in Mo$_6$Se$_8$, with two supplementary

(22) (a) Andersen, O. K. *Phys. Rev. B* **1975**, *12*, 3060. (b) Andersen, O. K. *Europhys. News* **1981**, *12*, 4. (c) Andersen, O. K. In *The Electronic Structure Of Complex Systems*; Phariseau, P., Temmerman, W. M., Eds.; Plenum Publishing Corporation: New York, 1984. (d) Andersen, O. K.; Jepsen, O. *Phys. Rev. Lett.* **1984**, *53*, 2571. (e) Andersen, O. K.; Jepsen, O.; Sob, M. In *Electronic Band Structure and its Application*; Yussouf, M., Ed.; Springer-Verlag: Berlin, 1986. (f) Skriver, H. L. *The LMTO Method*; Springer-Verlag: Berlin, 1984.
(23) von Barth, U.; Hedin, L. *J. Phys. C* **1972**, *5*, 1629.
(24) Jepsen, O.; Andersen, O. K. *Z. Phys. B* **1995**, *97*, 35.
(25) Blöchl, P. E.; Jepsen, O.; Andersen, O. K. *Phys. Rev. B* **1994**, *49*, 16223.
(26) Dronskowski, R.; Blöchl, P. E. *J. Phys. Chem.* **1993**, *97*, 8617.
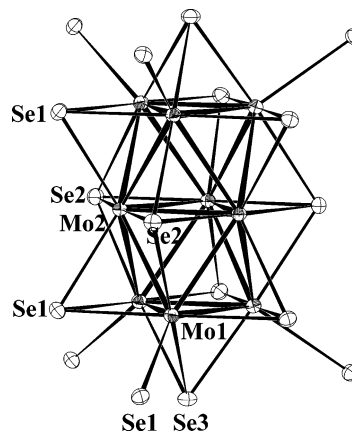(27) Jepsen, O.; Andersen, O. K. Personal communication.
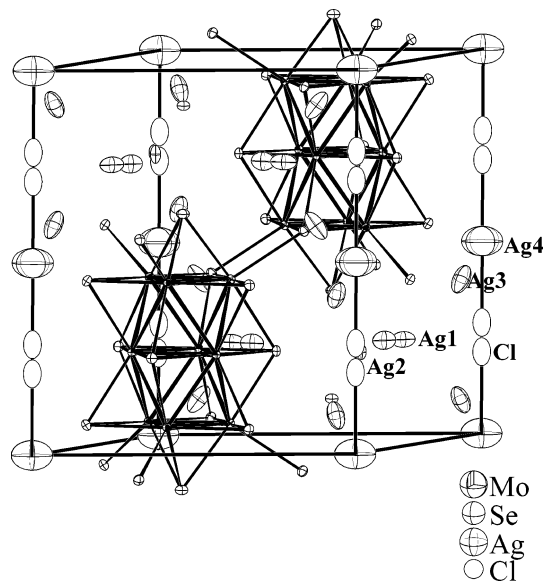
Figure 1. View of the crystal structure of $Ag_{4.1}ClMo_9Se_{11}$ (50% probability ellipsoids).

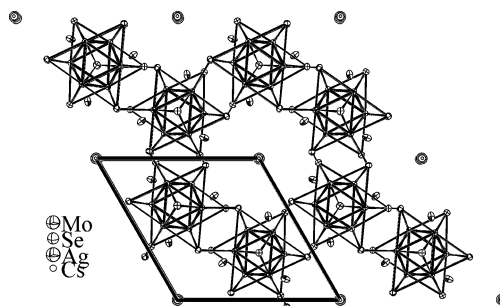**Figure 3.** The $Mo_9Se_5^iSe_{6/2}^{\ i-a}Se_{6/2}^{\ a-i}$ cluster unit (97% probability ellipsoids).

Figure 4. Projection of the crystal structure of $Ag_{2.6}CsMo_9Se_{11}$ onto the *ab* plane.

Figure 2. Joint probability density function (pdf) map for the Cs atoms in the ac plane in $Ag_{2.6}CsMo_9Se_{11}$ (min/max, 0/1693 Å^{-3}; step, 200 Å^{-3}).

chalcogen atoms capping the outer triangular faces. The outer Mo1 and the inner Mo2 atoms present different environments. Thus, the Mo1 atoms of the outer Mo_3 triangles have an environment similar to that encountered in the Mo_6X_8 units of the rhombohedral MMo_6X_8 (M = Na, Pb, RE, ...) (X = S, Se) compounds.[1] They are surrounded by four Mo atoms (two outer Mo1 and two inner Mo2) and four Se atoms, which are approximately coplanar, and another Se atom belonging to an adjacent Mo_9Se_{11} cluster and constitut-

ing the apex of a square based pyramidal environment. The Mo2 atoms of the median Mo_3 triangles are surrounded by six Mo atoms (four outer Mo1 and two inner Mo2) and only four Se atoms belonging to the same cluster unit. As observed in previous molybdenum condensed cluster chalcogenides,[9] two kinds of Mo−Mo distances can be distinguished in the units: the Mo−Mo intratriangle distances which correspond to the distances within the Mo_3 triangles formed by the Mo atoms related through the 3-fold axis and which vary between 2.6270(4) Å and 2.7423(6) Å and the Mo−Mo between the Mo_3 triangles that range from 2.6937(4) Å to 2.7985(5) Å. The Mo−Se bond distances are typical, with the shortest ones at about 2.52 Å and the longest ones at about 2.71 Å. Each unit is connected to six adjacent units via twelve interunit Mo1−Se1 bonds of about 2.71 Å (2.609 Å in **3**) to form a three-dimensional Mo−Se framework in which the shortest intercluster distance is around 3.64 Å in the quaternary phases and 3.22 Å in the binary. The connective formula of the Mo− Se network thus created is $[Mo_9Se5^iSe_{6/2}^{\ i-a}]Se_{6/2}^{\ a-i}$ in Schäfer's notation.[28] As shown by the projection of the structure onto the hexagonal plane (001) (Figure 4), it results from this arrangement that large channels extending along the *c* axis are created. They are occupied by a part of the silver atoms and the chlorine atoms in $Ag_{4.1}ClMo_9Se_{11}$ and by the caesium atoms in $Ag_{2.6}CsMo_9Se_{11}$. The others Ag atoms are located in a mirror plane around the 3-fold axis between two consecutive Mo_9Se_{11} units.

---

(28) Schäfer, H.; Von Schnering, H. G. *Angew. Chem.* **1964**, *20*, 833.
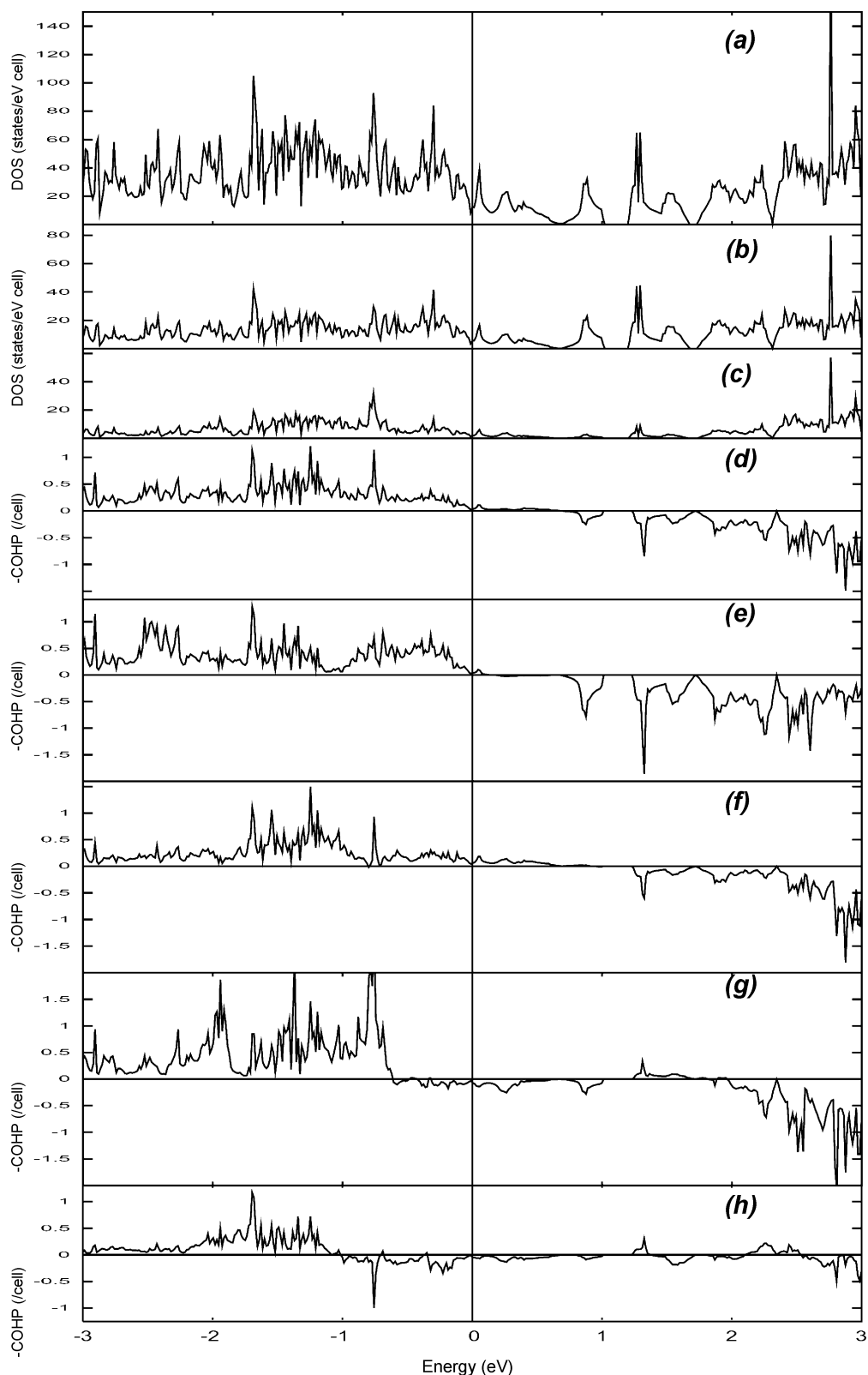
Figure 5. DFT calculations for h-Mo9Se11: (a) total DOS; (b) Mo1 projected DOS; (c) Mo2 projected DOS; (d) averaged Mo−Mo COHP of the Mo9Se11 cluster; (e) intracluster Mo1−Mo1 COHP; (f) intracluster Mo1−Mo2 COHP; (g) intracluster Mo2−Mo2 COHP; (h) intercluster Mo1−Mo1 COHP.

In $Ag_{4.1}ClMo_9Se_{11}$, four types of environment are observed for the silver atoms. The first one may be described as a distorted square based pyramid with Ag1−Se distances in the range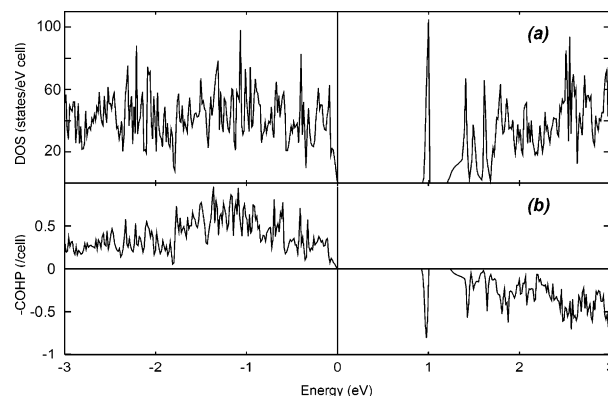 2.623(1)−3.005(3) Å. The second observed for Ag2 corresponds to a distorted tetrahedron formed by three Se (2.615(1) Å and 2 × 2.6864(6) Å) and one Cl (2.734(3) Å) atoms. The third coordination found for Ag3 consists of three Se at 2.761(5), 2.886(5), and 2.912(5) Å, and one Cl

atom at 2.623(7) Å in quasi-planar geometry. The atom Ag4 is two coordinated by the Cl atoms in a linear way with Ag−Cl distances of 2.516(7) Å.

In $Ag_{2.6}CsMo_9Se_{11}$, the unique crystallographically independent silver atoms occupy a site similar to that of Ag1 in $Ag_{4.1}ClMo_9Se_{11}$. The Cs cation is nine-coordinated by the Se atoms forming a tricapped triangular prism. The Cs−Se distances are in the range 3.679−3.986 Å.

Evolution of the Mo−Mo Distances. The most important difference in the three compounds investigated concerns the Mo−Mo intercluster distances which decrease from about 3.64 Å in the quaternary phases to 3.22 Å in the binary. Simultaneously, the Mo1−Mo1 distances within the ending Mo_3 triangle increase from 2.6270(4) Å to 2.6820(6) Å. This results principally from sterical effects. Another factor governing the Mo−Mo distances is the number of electrons per Mo_9 cluster. The latter effect is predominant in the Mo−Mo bonds within the median triangle and those between the Mo_3 triangles as shown previously.[14] Thus, an increase of the Mo−Mo bonds in the median triangle (2.6838(9) Å in **3**, 2.7362(5) Å in **2**, and 2.7423(6) Å in **1**) and a decrease of the distance between the median and ending triangles (2.294, 2.300, and 2.228 Å in **3**, **2**, and **1**, respectively) are observed when the metallic electron (ME) count per Mo_9 cluster increases (32 in **3**, 35.1 in **2**, and 35.6 in **1**).

Electronic Structure. Density functional calculations were carried out on h-Mo_9Se_{11} and on the model compound $Ag_3CsMo_9Se_{11}$. This latter is based on the crystal structure of $Ag_{2.6}CsMo_9Se_{11}$ where all silver atom positions are fully occupied. Hughbanks and Hoffmann have studied the electronic structure of the Mo_9S_{11} and $Mo_{12}S_{14}$ clusters.[29] On the basis of extended Hückel (EH) calculations, they proposed an optimal ME count of either 36 or 38 for the Mo_9S_{11} unit. Further DFT studies have shown that the ME count of 38 is unfavorable because the highest occupied molecular orbital (HOMO) is metal−metal antibonding overall and rather high in energy.[30] Mo_9 clusters showing a ME count closed to 36 have been characterized in $Ag_{3.6}Mo_9Se_{11}$[4] and $K_{1.8}Cu_2Mo_9S_{11}$.[12] This latter compound results from the insertion of copper by topotactic reduction−oxidation reaction in the $K_2Mo_9S_{11}$ compound. In the h-Mo_9Se_{11} compound, the ME count of the Mo_9Se_{11} cluster is equal to 32. Such a low electron count has been suggested for this cluster present with other clusters of different nuclearity in various compounds.[11] In the Fermi level region, total and projected DOS, and COHPs for several Mo−Mo atomic contacts resulting from first principles calculations for h-Mo_9Se_{11} are depicted in Figure 5. The Fermi level cuts a DOS peak mainly centered on Mo atoms. As shown by previous EHTB studies for similar compounds, Mo−Mo intercluster COHP indicates a weak but significant metal−metal bond between the clusters that is at the origin of the metallic behavior foreseen for h-Mo_9Se_{11}. EHTB study of $K_2Mo_9S_{11}$ has shown that its DOS presents two band gaps

(29) (a) Hughbanks, T.; Hoffmann, R. *J. Am. Chem. Soc.* **1983**, *105*, 1150. (b) Hughbanks, T. *Prog. Solid State Chem.* **1989**, *19*, 329.

(30) Gautier, R.; Gougeon, P.; Halet, J.-F.; Potel, M.; Saillard, J.-Y. *J. Alloys Compd.* **1997**, *262−263*, 311.

**Figure 6.** DFT calculations for $Ag_3CsMo_9Se_{11}$: (a) total DOS; (b) averaged Mo−Mo COHP of the Mo_9Se_{11} cluster.
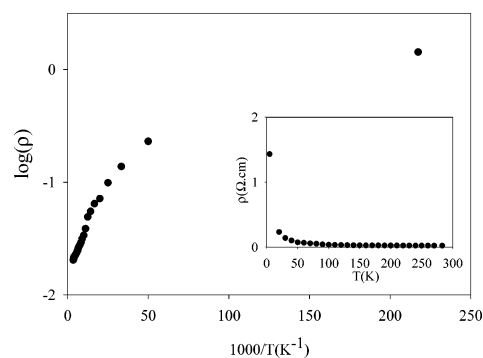
Figure 7. Arrhenius plot for $Ag_{2.6}CsMo_9Se_{11}$. Inset shows the temperature dependence of the resistivity.

for electron counts that correspond to 36 and 38 ME for the Mo_9S_{11} cluster. For h-Mo_9Se_{11}, one band gap for 38 ME lies around ca. 1 eV (cf. Figure 5a). On the other hand for the ME count of 36 (around ca. 0.7 eV) such a band gap is not present for the selenide cluster. Mo−Mo COHPs shows that the ME count of 36 implies the occupation of all metal−metal bonding bands. Bands that lie above the Fermi level and below 0.7 eV are mainly located on the outer Mo1 atoms. These bands show an overall weakly Mo−Mo bonding character. Assuming a rigid band model, addition of 4 extra electrons per Mo_9 unit should be possible without altering the structural arrangement much. The intracluster Mo1−Mo2 distance should slightly shorten whereas intracluster Mo2−Mo2 and intercluster Mo−Mo distances should slightly lengthen when electrons are added. As mentioned above, this evolution is experimentally observed when crystal structures of $Ag_{2.6}CsMo_9Se_{11}$, $Ag_{4.1}ClMo_9Se_{11}$, and h-Mo_9Se_{11} are compared. Total and projected DOS, and COHPs for Ag−Mo2 and the whole Mo−Mo atomic contacts resulting from first principles calculations for the model compound $Ag_3CsMo_9Se_{11}$ are depicted in Figure 6. A large band gap of ca. 1 eV separates the Mo−Mo bonding and nonbonding bands from the Mo−Mo antibonding bands. The vacant DOS peak centered around 1 eV that would be occupied for the ME count of 38 on the Mo_9 cluster shows an Mo−Mo antibonding character. Therefore, the ME count of 38 is unfavorable. Integrated COHP values indicate that Mo−Mo intercluster bonding is not significant (−0.011 Ry/cell) whereas Ag−Mo2 bond strength (−0.063 Ry/cell) is more
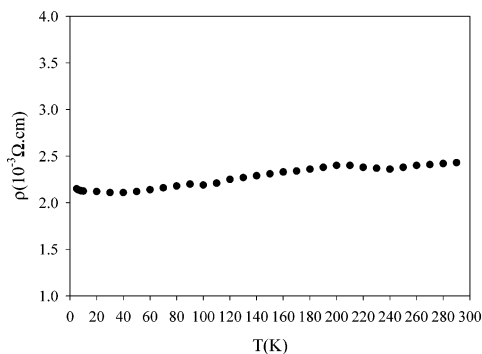
Figure 8. Temperature dependence of the resistivity of a single crystal of $Ag_{4.1}ClMo_9Se_{11}$.

than one-third of the averaged intracluster metallic bond strength (-0.169 Ry/cell). If a rigid band model is assumed, metallic properties for $Ag_{2.6}CsMo_9Se_{11}$ can be expected as well as for $Ag_{4.1}ClMo_9Se_{11}$ owing to the strong similarity of their crystal structures. However, because of the partial occupation of some silver atoms, further calculations with a larger unit cell would be necessary in order to expect confident predictions of their conductivity properties. Moreover the long intercluster Mo−Mo distance in these compounds must have a significant influence on the electrical conductivity.

Resistivity Properties. Variable-temperature resistivity data for single crystals of $Ag_{2.6}CsMo_9Se_{11}$ and $Ag_{4.1}Cl$-Mo_9Se_{11} in the temperature range 4−290 K are presented in Figures 7 and 8, respectively. $Ag_{4.1}ClMo_9Se_{11}$ exhibits semimetallic behavior with a resistivity quasi-independent

of the temperature and a room temperature resistivity of 2.4 $\times 10^{-3}$ Ω cm. $Ag_{2.6}CsMo_9Se_{11}$ presents a semiconducting behavior with a resistivity of 2.0 $\times 10^{-2}$ Ω cm at room temperature and an activation energy of 6.5×10^{-3} eV. It is interesting to note that the orthorhombic phase $Ag_{3.6}Mo_9$-Se_{11} that has 35.6 MEs/Mo_9 unit as in $Ag_{2.6}CsMo_9Se_{11}$ is a semiconductor. Due to the lack of suitable large single crystals of h-Mo_9Se_{11}, no resistivity measurement was made. However, theoretical calculations suggest that a metallic behavior is expected as for the isoelectronic compound, o-Mo_9Se_{11},[13] that is obtained by the silver deinsertion from the orthorhombic phase $Ag_{3.6}Mo_9Se_{11}$.

Conclusion

In this work, we have presented the three new isostructural compounds $Ag_{2.6}CsMo_9Se_{11}$, $Ag_{4.1}ClMo_9Se_{11}$, and h-Mo_9Se_{11} that were synthesized either by solid-state or by oxido−reduction reaction. Single-crystal X-ray diffraction studies showed that their structures contain quasi-isolated Mo_9Se_{11} units forming an original three-dimensional network in which large channels are observed. The framework Mo_9Se_{11} seems to be particularly adapted for topotactic reaction by "chimie douce". Further work is in progress to insert other cations in the channels.